



UNIVERSITY OF LEEDS

This is a repository copy of *Non-Linear Dynamic Behaviour of a Masonry Arch Subjected to Hinge Control*.

White Rose Research Online URL for this paper:
<http://eprints.whiterose.ac.uk/149954/>

Version: Accepted Version

Proceedings Paper:

Stockdale, G, Sarhosis, V orcid.org/0000-0002-8604-8659 and Milani, G (2019) Non-Linear Dynamic Behaviour of a Masonry Arch Subjected to Hinge Control. In: Papadrakakis, M and Fragiadakis, M, (eds.) Proceedings of the 7th International Conference on Computational Methods in Structural Dynamics and Earthquake Engineering (COMPDYN 2019). 7th International Conference on Computational Methods in Structural Dynamics and Earthquake Engineering (COMPDYN 2019), 24-26 Jun 2019, Crete, Greece. Ecomas Proceedia , pp. 1242-1250. ISBN 978-618-82844-6-3

<https://doi.org/10.7712/120119.6993.18761>

© 2019 The Authors. This is an author produced version of a paper published in Proceedings of the 7th International Conference on Computational Methods in Structural Dynamics and Earthquake Engineering (COMPDYN 2019).

Reuse

Items deposited in White Rose Research Online are protected by copyright, with all rights reserved unless indicated otherwise. They may be downloaded and/or printed for private study, or other acts as permitted by national copyright laws. The publisher or other rights holders may allow further reproduction and re-use of the full text version. This is indicated by the licence information on the White Rose Research Online record for the item.

Takedown

If you consider content in White Rose Research Online to be in breach of UK law, please notify us by emailing eprints@whiterose.ac.uk including the URL of the record and the reason for the withdrawal request.



eprints@whiterose.ac.uk
<https://eprints.whiterose.ac.uk/>

NON-LINEAR DYNAMIC BEHAVIOUR OF A MASONRY ARCH SUBJECTED TO HINGE CONTROL

Gabriel Stockdale¹, Vasilis Sarhosis², and Gabriele Milani²

¹ Dept. of Architecture, Built Environment and Construction Engineering, Politecnico di Milano
Piazza Leonardo da Vinci 32, 20133 Milan, Italy
e-mail: {gabriellee.stockdale, gabriele.milani}@polimi.it

² School of Engineering, University of Leeds
LS2 9JT, UK
v.sarhosis@leeds.ac.uk

Abstract

Masonry arches are vulnerable to seismic actions. Over the last few years, extensive research has been carried out to develop strategies and methods for their strengthening. However, from such studies, it became evident that the application of reinforcement in a masonry arch is done in such a manner that the failure of the system is transformed directly from one of stability to strength. This direct transformation overlooks the intermittent stages that exist between stability and strength, and thus provides an incomplete picture to the potential behaviors of the system. This study aims to investigate the non-linear dynamic behavior of masonry arches subjected to hinge control through the two-dimensional Discrete Element Method (DEM) based software UDEC. Within the DEM, each voussoir of the arch was represented by a distinct block. Mortar joints were modelled as zero thickness interfaces which can open and close depending on the magnitude and direction of the stresses applied to them. Twenty-five unique configurations of an arch with controlled hinges were developed and their behavior to different ground shaking motions is discussed. From the results of this analysis, it is evident that controlling the hinges of a masonry arch creates the potential to both increase capacity and define failure for dynamic loading conditions.

Keywords: Masonry, arches, hinges, strengthening, earthquakes

1 INTRODUCTION

Reinforcement of masonry arches is critical for resisting seismic induced collapse. Of all the existing techniques, fiber reinforced polymers (FRP) and textile reinforced mortars (TRM) both focus on reinforcing the development of flexural joints. Their application is typically designed to maximize capacity which transforms the arch's failure from the traditional minimum mechanism to a material strength problem (i.e. delamination, rupture or crushing) [1-8]. Considering the intermittent stages between the minimum mechanism and full strengthening under static assessments has revealed the potential to both increase seismic capacity and control failure for arches subjected to hinge control [9-11]. It is now necessary to begin expanding the evaluation beyond the static conditions. This work presents the numerical examination of a class of admissible mechanisms for a dry-stack masonry arch subjected to hinge control.

2 ARCH MODEL

A 27-block semicircular arch model was used for this investigation.

2.1 Arch Geometry

The arch and block geometry can be seen in Fig. 1 and its nomenclature used in Fig. 2.

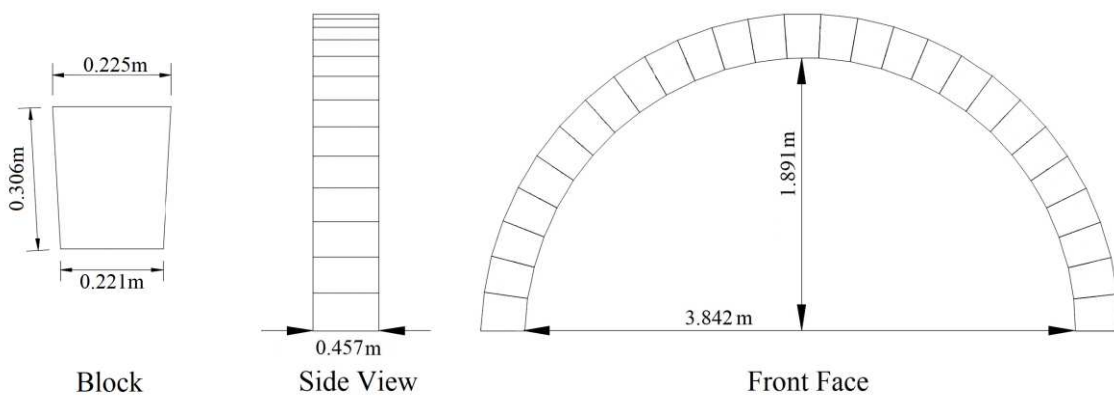


Figure 1: 27-block arch analysis model geometry and block dimensions

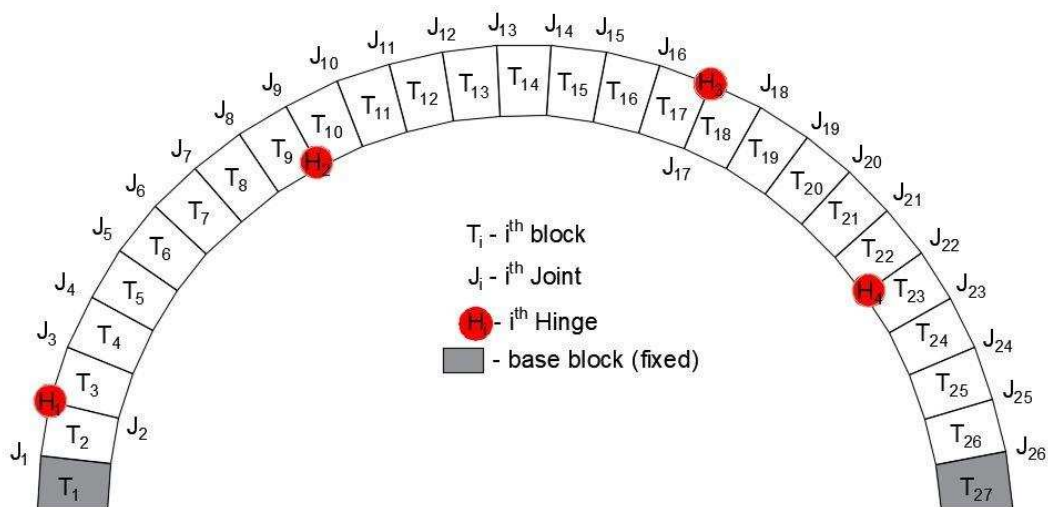


Figure 2: Nomenclature for arch model

2.2 Overview of DEM and Model Development

For the analysis of the arch presented in Section 2, the discrete element method of analysis have been employed. The discrete element method (DEM) falls within the general classification of discontinuum analysis techniques. It is presented in the UDEC (Universal Distinct Element Code) software, developed by Cundall in the early 1970s for numerical research into the sliding of earth and rock masses. Since then, the software has been used for a range of applications including the modelling of classical columns under static and dynamic loading conditions. In UDEC, masonry units are represented as an assembly of rigid or deformable blocks which may take any arbitrary geometry. Rigid blocks do not change their geometry as a result of any applied loading. Deformable blocks are internally discretised into finite difference triangular zones of uniform stress and strain characteristics. These zones are continuum elements as they occur in the finite element method (FEM). However, unlike FEM, in the DEM a compatible finite element mesh between the blocks and the joints is not required. Mortar joints are represented as zero thickness interfaces between the blocks. Representation of the contact between blocks is not based on joint elements, as occurs in the discontinuum finite element models. Instead the contact is represented by a set of point contacts with no attempt to obtain a continuous stress distribution through the contact surface. The assignment of contacts allows the interface constitutive relations to be formulated in terms of the stresses and relative displacements across the joint. As with FEM, the unknowns are the nodal displacements and rotations of the blocks. However, unlike FEM, the unknowns in the distinct element method are solved explicitly by differential equations from the known displacement while Newton's second law of motion gives the motion of the blocks resulting from known forces acting on them. So, large displacements and rotations of the blocks are allowed with the sequential contact detection and the automatic update of tasks. This differs from FEM where the method is not readily capable of updating the contact size or creating new contacts. Convergence to static solutions is obtained by means of adaptive damping, as in the classical dynamic relaxation methods.

A control arch model and interdependent geometric models to evaluate each variation in hinge positions tested were developed. The control arch contained no hinge control and was modelled by 27 rigid voussoirs connected by 26 joint interfaces (see Fig. 3). For a defined mechanical joint set, the arch was represented by three rigid voussoirs, two rigid bases and four joints as shown in Fig. 3. All joints were defined as zero-thickness interface elements that follow the Coulomb failure criterion. A description of modelling masonry with DEM can be found at [14, 15].

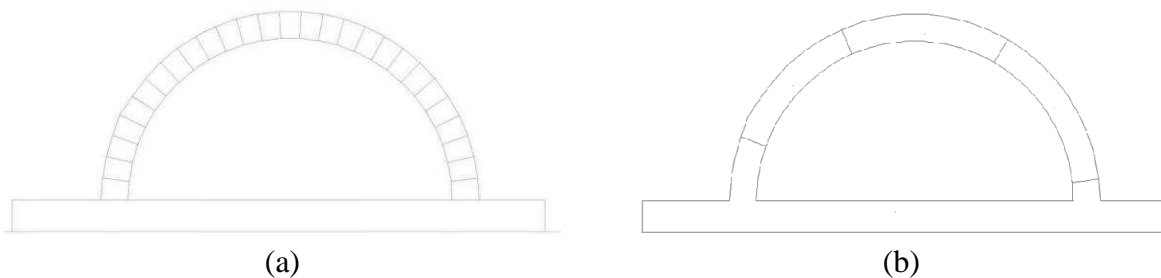


Figure 3: Geometry for the (a) control arch DEM model and (b) a typical hinge-controlled DEM model.

The material properties assigned to the voussoirs of each arch ring are shown in Table 1. The material parameter required to represent the behavior of the rigid voussoirs is the unit weight (d), which was taken as 550 kg/m^3 . Elastic-perfectly plastic coulomb slip joint area

contact interfaces were used for the joints between voussoirs. The normal and shear stiffness for the joints were selected high to remove potential penetration between blocks. The cohesive, tensile strength and the dilatation angle of the interfaces were set to zero to represent dry-joints. Self-weight effects were also modelled as gravitational loads.

Joint Normal Stiffness [GPa/m]	Joint Shear Stiffness [GPa/m]	Joint Friction Angle [°]	Joint Cohesive Strength [kPa]	Joint Tensile Strength [MPa]	Joint Dilation Angle [°]
20	10	22	0	0	0

Table 1: Material Properties for the dry-joints in the DEM models.

Self-weight effects were assigned as gravitational load. At first, the model was brought into a state of equilibrium under its own weight (static gravity loads). Then, external loading has been applied to the structure by applying a time history analysis, see Section 3.1. Horizontal displacements at the upper part of the arch were recorded. The results of the response of the structure under dynamic load is presented below.

3 ANALYSIS PROCEDURE

The dynamic analysis procedure for this investigation involved a two-stage process. First, the dynamic ground velocity profile was applied to the free-standing arch without hinge control to establish a collapse time. The collapse time was then used to test the 25 unique hinge sets established through hinge control at a scale of one, two, three, four and five times the original. For each simulation, the arch was allowed to rest after the collapse time to establish a final settlement condition. The crown and base displacements were recorded. The final settled horizontal displacement of the crown was compared for each hinge set and earthquake scale. From that comparison, the optimal hinge configuration was identified by the hinge set with the minimum final deformation. The second analysis stage involved the application of the full earthquake duration to the identified optimal hinge configuration and examine any adjustments required to resist collapse.

3.1 Earthquake Data

The ground velocity vector from Bucharest 1977 earthquake (see Fig. 4) was applied in both the horizontal and vertical directions for each analysis run. The scale of the vectors was adjusted for some analyses between one and five times the original.

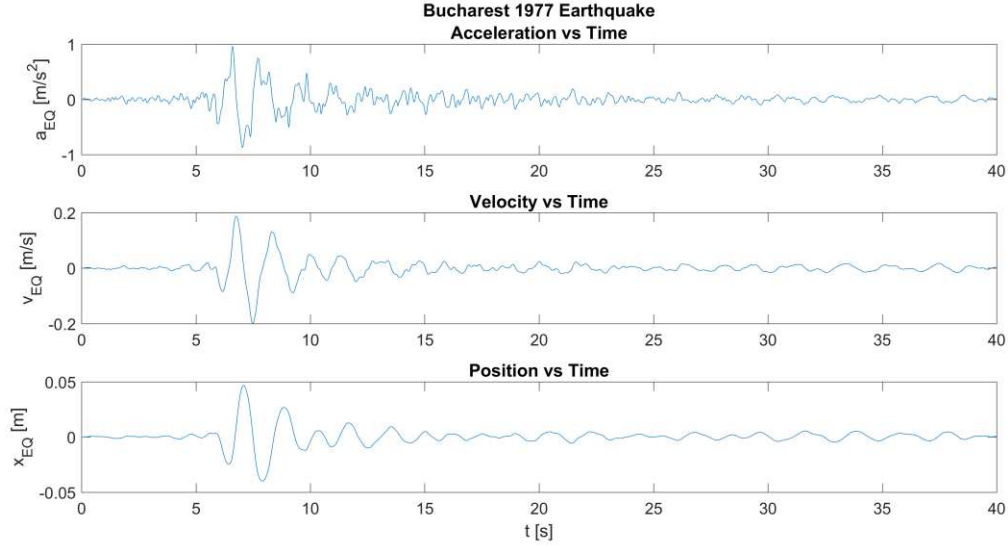


Figure 4: Acceleration, velocity and position profiles for the Bucharest 1977 earthquake.

3.2 Hinge Sets

Tables 2 through 4 identify the 25 distinct hinge sets tested. The selected hinge sets are the minimum configurations for the admissible locations of base hinges (H_1 and H_4). They were determined through the development of a collapse load diagram for the arch subjected to constant horizontal acceleration [12].

	HS01	HS02	HS03	HS04	HS05	HS06	HS07	HS08	HS09	HS10
H_1	J_1	J_1	J_1	J_1	J_1	J_2	J_2	J_2	J_2	J_2
H_2	J_8	J_8	J_8	J_8	J_8	J_8	J_9	J_9	J_9	J_9
H_3	J_{17}	J_{17}	J_{16}	J_{16}	J_{16}	J_{16}	J_{17}	J_{17}	J_{17}	J_{18}
H_4	J_{26}	J_{25}	J_{24}	J_{23}	J_{22}	J_{22}	J_{23}	J_{24}	J_{25}	J_{26}

Table 2: Hinge joint locations for hinge sets HS01 through HS10. Refer to Fig. 2 for joint identification.

	HS11	HS12	HS13	HS14	HS15	HS16	HS17	HS18	HS19	HS20
H_1	J_3	J_3	J_3	J_3	J_3	J_4	J_4	J_4	J_4	J_4
H_2	J_{10}	J_{10}	J_{10}	J_9	J_9	J_{10}	J_{10}	J_{10}	J_{11}	J_{11}
H_3	J_{17}	J_{17}	J_{16}	J_{16}	J_{16}	J_{16}	J_{17}	J_{17}	J_{17}	J_{18}
H_4	J_{26}	J_{25}	J_{24}	J_{23}	J_{22}	J_{22}	J_{23}	J_{24}	J_{25}	J_{26}

Table 3: Hinge joint locations for hinge sets HS11 through HS20. Refer to Fig. 2 for joint identification.

	HS21	HS22	HS23	HS24	HS25
H_1	J_3	J_3	J_3	J_3	J_3
H_2	J_{10}	J_{10}	J_{10}	J_9	J_9
H_3	J_{17}	J_{17}	J_{16}	J_{16}	J_{16}
H_4	J_{26}	J_{25}	J_{24}	J_{23}	J_{22}

Table 4: Hinge joint locations for hinge sets HS21 through HS25. Refer to Fig. 2 for joint identification.

4 RESULTS

4.1 Unreinforced Collapse Time

The unreinforced collapse time was defined as the time at which the keystone struck the ground. This time is 5.7 seconds and was identified from the vertical displacement versus time plot shown in Fig. 5. Figure 5 also shows the final condition of the unreinforced arch.

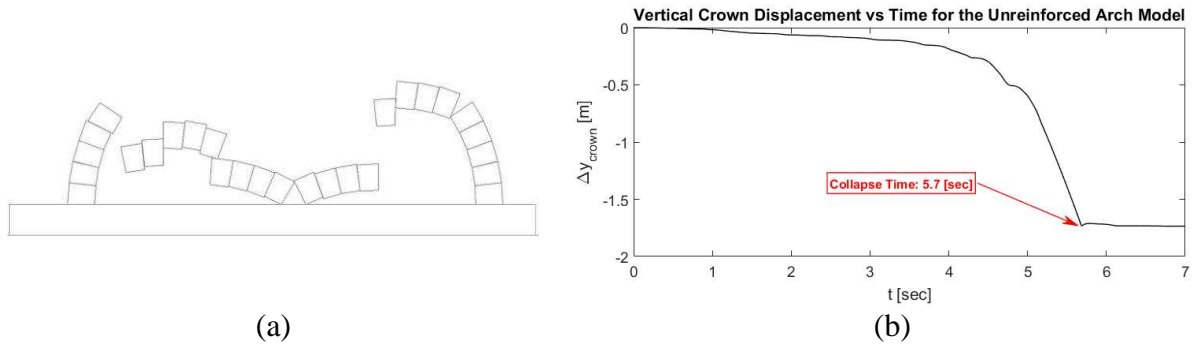


Figure 5: The (a) collapsed unreinforced arch and (b) collapse time identification plot.

4.2 Optimal Hinge Set Identification

None of the arch models subjected to hinge control collapsed over the established collapse time duration. Sliding did occur however and was therefore used to establish an evaluation criterion for determining the optimal hinge configuration for the arch under investigation. Figure 6 shows the final horizontal crown displacement versus hinge set for all analyses performed. From Fig. 6, hinge set 05 resulted in the minimum deformations and is identified as the optimal hinge set configuration. Figure 7 shows a generalized reinforcement layout that would produce the hinge set 05 condition.

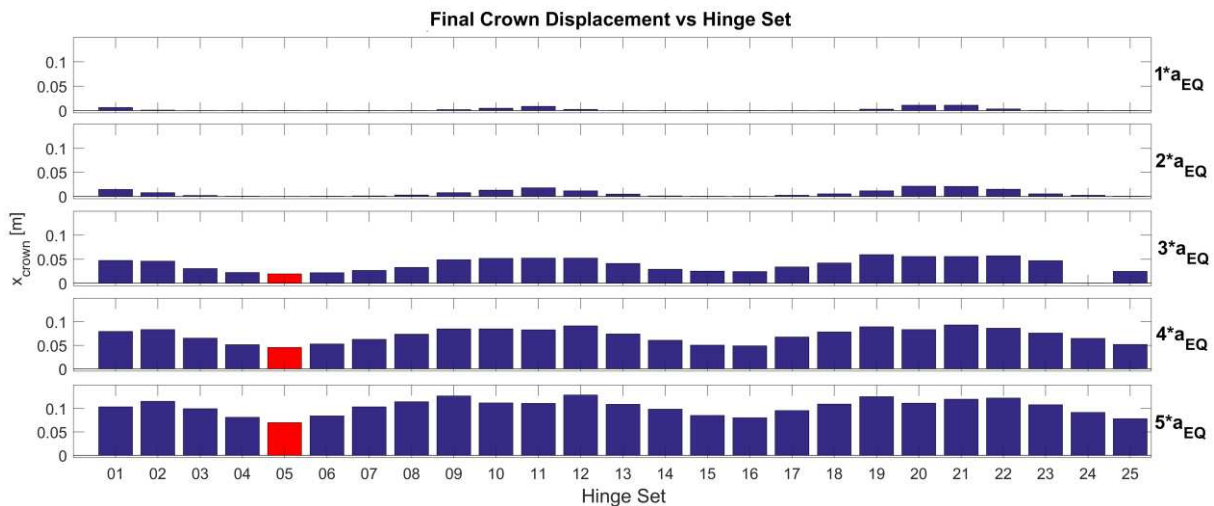


Figure 6: Final horizontal displacement versus hinge sets for all scaled dynamic analyses performed for the collapse time duration.

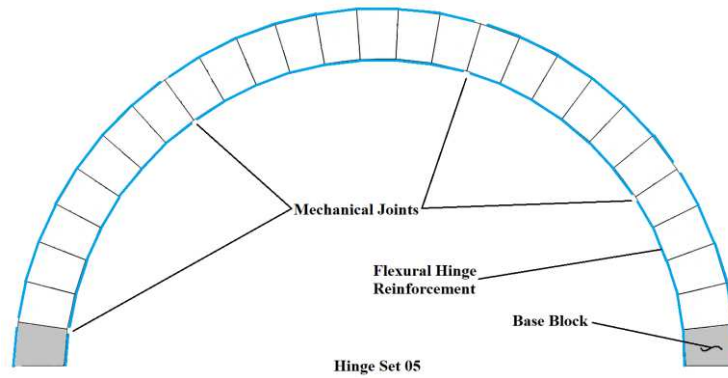


Figure 7: Hinge set 05 reinforcement layout

4.3 Hinge Set 05 Performance

The application of the full earthquake duration to the identified optimum hinge configuration revealed a total collapse of the arch at 13.12 seconds (see Fig. 8). However, increasing the friction angle of the model from 22° to 50° resulted in an arch that did not fail from the original or double scaled dynamic condition as can be seen in Fig. 9.

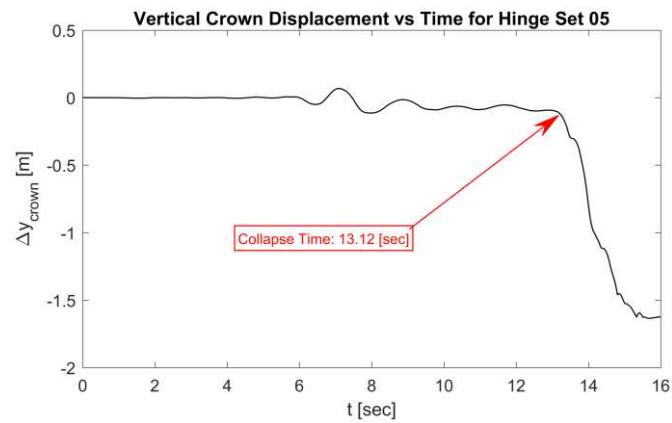


Figure 8: Collapse time identification for hinge set 05.

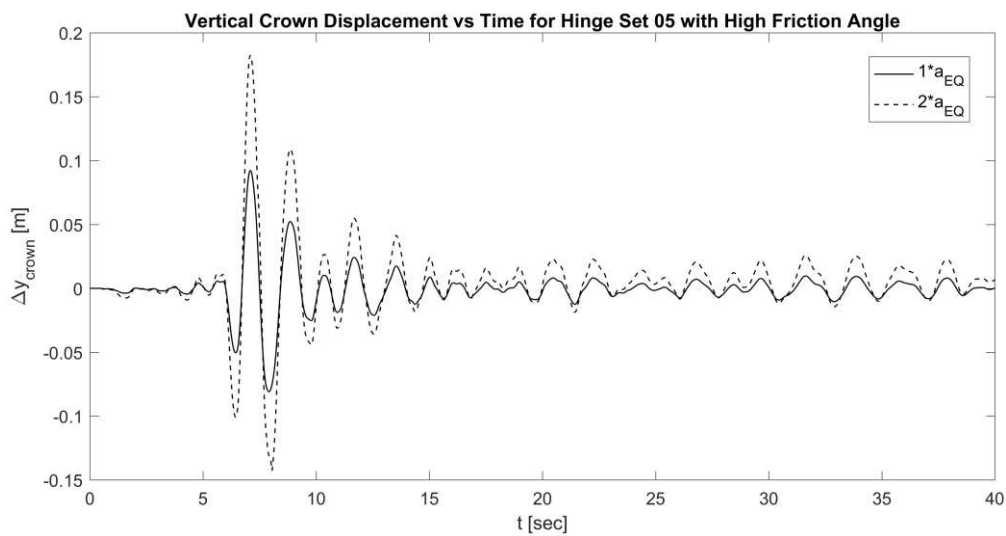


Figure 9: Vertical crown displacement versus time for hinge set 05 with a high friction angle.

5 CONCLUSIONS

The Reinforcement of masonry arches is critical for resisting seismic collapse. This work presented the numerical examination of a class of admissible mechanisms for a dry-stack masonry arch subjected to hinge control. From the analyses the increase in performance is directly observed for all hinge-controlled conditions, but it was also observed that removal of slip is as important as defining the joints for obtaining the best performance.

REFERENCES

- [1] E. Bertolesi, G. Milani, F.G. Carozzi, C. Poggi, Ancient masonry arches and vaults strengthened with TRM, SRG and FRP composites: Numerical analyses. *Composite Structures*, **187**, 385-402, 2018.
- [2] F.G. Carozzi, C. Poggi, E. Bertolesi, G. Milani, Ancient masonry arches and vaults strengthened with TRM, SRG and FRP composites: Experimental evaluation. *Composite Structures*, **187**, 466-480, 2018.
- [3] S. De Santis, F. Roscini, G. de Felice, Full-scale tests on masonry vaults strengthened with Steel Reinforced Grout. *Composites Part B*, **141**, 20-36, 2018.
- [4] L. Anania, G. D'Agata, Limit Analysis of vaulted structures strengthened by an innovative technology in applying CFRP. *Construction and Building Materials*, **145**, 336-346, 2017.
- [5] C. Modena, G. Tecchio, C. Pellegrino, F. da Porto, M. Donà, P. Zampieri, M.A. Zanini, Reinforced concrete and masonry arch bridges in seismic areas: typical deficiencies and retrofitting strategies. *Structure and Infrastructure Engineering*, **11**:4, 415-442, 2015.
- [6] A. Borri, G. Castori, M. Corradi, Intrados strengthening of brick masonry arches with composite materials. *Composites: Part B*, **42**, 1164-1172, 2011.
- [7] I. Cancelliere, M. Imbimbo, E. Sacco, Experimental tests and numerical modelling of reinforced masonry arches. *Eng Struct*, **32**, 776-792, 2010.
- [8] D.V. Oliveira, I. Basilio, P.B. Lourenço, Experimental Behavior of FRP Strengthened Masonry Arches, *J. Compos. Constr.*, **14**:3, 312-322, 2010.
- [9] G. Stockdale, V. Sarhosis, G. Milani, Increase in seismic resistance for a dry joint masonry arch subjected to hinge control, 10th IMC Conference Proceedings, International Masonry Society, 968-981, 2018.
- [10] G. Stockdale, V. Sarhosis, G. Milani, Seismic Capacity and Multi-Mechanism Analysis for Dry-Stack Masonry Arches Subjected to Hinge Control, *Bull Earthq Eng*, 2019.
- [11] G. Stockdale, G. Milani, V. Sarhosis, Increase in Seismic Resistance for a Full-Scale Dry Stack Masonry Arch Subjected to Hinge Control, *Key Engineering Materials*, (In press)
- [12] G. Stockdale, G. Milani, Diagram based assessment strategy for first-order analysis of masonry arches, *J. Building Engineering*, **22**, 122-129, 2019.
- [13] V. Sarhosis, K. Bagi, J.V. Lemos, G. Milani. (2016). *Computational modeling of masonry structures using the discrete element method*. IGI Global, USA.

- [14] V. Sarhosis, Sheng Y. Identification of material parameters for low bond strength masonry, *Engineering Structures*, **60**, 100-110, 2014.